

# The Atmospheres of Extrasolar Super-Earths

Eliza Miller-Ricci<sup>1</sup>, Sara Seager<sup>2</sup>, and Dimitar Sasselov<sup>1</sup>

<sup>1</sup>Harvard Smithsonian Center for Astrophysics  
60 Garden St., Cambridge, MA 02138

email: [emillerricci@cfa.harvard.edu](mailto:emillerricci@cfa.harvard.edu), [sasselov@cfa.harvard.edu](mailto:sasselov@cfa.harvard.edu)

<sup>2</sup>Department of Earth, Atmospheric, and Planetary Sciences, Department of Physics,  
Massachusetts Institute of Technology  
54-1626, 77 Massachusetts Ave., Cambridge, MA 02139  
email: [seager@mit.edu](mailto:seager@mit.edu)

**Abstract.** Extrasolar super-Earths (1-10  $M_{\oplus}$ ) are likely to exist with a wide range of atmospheres. While a number of these planets have already been discovered through radial velocities and microlensing, it will be the discovery of the first *transiting* super-Earths that will open the door to a variety of follow-up observations aimed at characterizing their atmospheres. Super-Earths may fill a large range of parameter space in terms of their atmospheric composition and mass. Specifically, some of these planets may have high enough surface gravities to be able to retain large hydrogen-rich atmospheres, while others will have lost most of their hydrogen to space over the planet's lifetime, leaving behind an atmosphere more closely resembling that of Earth or Venus. The resulting composition of the super-Earth atmosphere will therefore depend strongly on factors such as atmospheric escape history, outgassing history, and the level of stellar irradiation that it receives. Here we present theoretical models of super-Earth emission and transmission spectra for a variety of possible outcomes of super-Earth atmospheric composition ranging from hydrogen-rich to hydrogen-poor. We focus on how observations can be used to differentiate between the various scenarios and constrain atmospheric composition.

---

## 1. Introduction

The search for extrasolar planets has recently resulted in the discovery of a new class of planets, super-Earths, with masses between 1 and 10 Earth masses ( $M_{\oplus}$ ) (Rivera *et al.* 2005; Beaulieu *et al.* 2006; Udry *et al.* 2007). Since no such planets exist in our Solar System, the bulk composition of these planets and of their atmospheres remains largely unknown. In contrast to rocky planets in our Solar System, super-Earths are predicted to have large surface gravities, (Valencia *et al.* 2007; Fortney *et al.* 2007; Seager *et al.* 2007; Sotin *et al.* 2007) and some of these planets may be able to retain massive H-rich atmospheres. Others will bear a closer resemblance to Earth, with atmospheres depleted in hydrogen and composed of predominantly heavier molecules. A third interesting case is that some super-Earths may lie in between these two extremes, with moderate levels of atmospheric hydrogen due to incomplete escape of hydrogen over the planet's lifetime and/or outgassing of a significant initial  $H_2$  atmosphere. The question arises as to whether these cases will differ in their gross observable properties, and how. In the interest of discovering habitable planets and learning more about atmospheric evolution on Super-Earths, it will be necessary to find a method for discriminating between the possible types of atmospheres. This issue has led us to model the observational signature for the various possible atmospheres on the lowest-mass planet presented in the literature to date, Gl 581c (Udry *et al.* 2007). The cases that we explore are (i) a massive hydrogen-rich (reducing) atmosphere obtained through accretion of nebular gas, (ii) a mildly reducing atmosphere that has lost most but not all of its hydrogen due

to atmospheric escape processes, and (iii) an oxidizing CO<sub>2</sub>-rich atmosphere similar in composition to that of Venus that contains essentially no hydrogen. From the modeled spectra, we determine how to observationally differentiate between the various scenarios.

## 2. Super Earth Atmosphere Model

### 2.1. Opacities

We determine molecular opacities following the procedure outlined in Seager *et al.* (2000) for wavelengths ranging from 0.1 to 100  $\mu\text{m}$ . We include the dominant sources of molecular line opacity in the IR: CH<sub>4</sub>, CO, NH<sub>3</sub>, (Freedman *et al.* 2007, and references therein), H<sub>2</sub>O (Freedman *et al.* 2007; Partridge & Schwenke 1997), CO<sub>2</sub>, O<sub>2</sub>, and O<sub>3</sub> (Rothman *et al.* 2005), as well as CO<sub>2</sub> - CO<sub>2</sub> collision induced opacities (Brodbeck *et al.* 1991), which we find to have an effect on the near-IR portion of some of the super-Earth spectra.

### 2.2. Chemistry

Given the atomic makeup of our super-Earth atmosphere, we determine molecular abundances in chemical equilibrium. This is accomplished by minimizing Gibbs free energy following the method outlined in White *et al.* (1958) for 23 atoms and 172 gas phase molecules. We do not include a full treatment of condensed species in our chemical model, although we do check whether any of our model atmospheres cross the condensation curves of known cloud-forming species.

After completing the chemical equilibrium calculation and determining the atmospheric temperature-pressure profile (§ 2.3), we take the following additional steps to account for the major effects of ammonia and methane photochemistry. We calculate photolysis lifetimes for each of these species, and the molecule is determined to be photochemically unstable if its lifetime is found to be significantly smaller than the age of the planet (approximately 4.3 Gyr; Udry *et al.* 2007). If this is the case, we then remove the unstable molecule from our chemical equilibrium calculation, and its atomic constituents are then reallocated to molecules that are stable against photodissociation. We do not calculate the full networks of chemical reactions for NH<sub>3</sub> and CH<sub>4</sub>, but we assume that return reactions for both of these species occur far more slowly than photolysis.

### 2.3. Irradiated Temperature-Pressure Profile

We compute a 1-D radial temperature-pressure (T-P) profile for Gl 581c. We make the assumption of an irradiated grey atmosphere (Chevallier *et al.* 2007; Hansen 2007) in hydrostatic equilibrium. In regions where the atmosphere is found to be convectively unstable we switch from the grey temperature profile to an adiabatic profile with the appropriate lapse rate. While this is an overly simplistic approach for calculating the T-P profile, we point out that the major results we present in this proceedings are not strongly dependent on the exact T-P profile that is used.

### 2.4. Atmospheric Mass

The mass of Gl 581c's atmosphere is one of the major unknowns involved in our model. In our own Solar System, the atmospheric masses of similarly-sized Earth and Venus vary by almost two orders of magnitude, which implies that other factors such as formation history or the presence of liquid oceans have a large effect on this parameter. Regardless of this, we find that the results we present in this paper have little dependence on the mass of the atmosphere. Since no transit observations exist for Gl 581c to constrain the

planet's density, we must therefore assume values for atmospheric mass in our models. In Section 3 we discuss our choices.

### 2.5. Emission and Transmission Spectra

To determine the planet's emitted spectrum, we integrate the equation of transfer through the planet's atmosphere using the T-P profile as outlined in Section 2.3. We include the effects of Rayleigh scattering but not the effects of aerosols or photochemical hazes.

For the transmission spectra we once again integrate the transfer equation through the planet's atmosphere, but here we only include absorption and Rayleigh scattering out of the beam. We integrate over the slant optical depth through the atmosphere in order to account for the viewing geometry in transit. To calculate transmission spectra, it is also necessary to assume a planetary radius,  $R_p$ , both to determine the amount of stellar flux that is blocked out during transit as well as for computing path lengths through the planet's atmosphere. Since Gl 581c has not been found to transit, we rely on theoretical predictions of the mass-radius relationship for super-Earths. We choose a radius of  $1.4 R_{\oplus}$ , corresponding to a rocky planet with a composition similar to Earth, composed of 67.5% silicate mantle and 32.5% iron core (Seager *et al.* 2007; Valencia *et al.* 2007).

## 3. Atmospheric Composition

The formation history of Gl 581c is largely unknown, and similarly, the mechanism by which the planet obtained its atmosphere remains uncertain. In particular, for the terrestrial planets in our Solar System, the issue of atmospheric escape plays a central role in our understanding of these planets' histories. From a simple thermal escape point of view, we find that Gl 581c lies in an interesting region of parameter space where it is unclear whether the planet is able to retain hydrogen over its lifetime. However, a variety of nonthermal escape processes can proceed at faster rates and are more difficult to constrain (Hunten *et al.* 1989). As a further complication, the initial amount of outgassing of hydrogen and other gasses from the planetary surface is almost entirely unconstrained, making it difficult to ascertain how hydrogen loss would contribute to the present atmospheric composition (Elkins-Tanton & Seager 2008).

For this reason, and in order to present results of more general relevance, we choose to model three distinctly different atmospheres for Gl 581c. These vary in their composition and in the ways by which they would be acquired by the planet. The three cases that we choose also span the range from hydrogen-rich to hydrogen-poor in our effort to understand the different observational signatures of these types of atmospheres. The scenarios are outlined as follows, and their atomic compositions are listed in Table 1.

### I. Hydrogen-Rich Atmosphere

Our first model atmosphere is composed predominantly of hydrogen (73.2% by mass). This atmosphere represents one obtained through a standard accretion process that has experienced little evolution later in its lifetime. This results in a reducing chemistry where hydrogen-bearing molecules dominate the atmosphere. The chemical equilibrium calculations result in a composition of mostly  $H_2$ , along with significant quantities of  $H_2O$ ,  $CH_4$ , and  $NH_3$ . However, due to photochemical considerations, the methane and ammonia are most likely destroyed. We therefore present two cases in the following sections - one with  $NH_3$  and  $CH_4$  at their equilibrium abundances and one with these species removed from the model. We employ an atmospheric mass for this model that is scaled up by a factor of 4 compared to that of the Earth, to account for the large quantity of hydrogen that remains in this atmosphere.

**Table 1.** Atomic Composition

Species	H-Rich	Intermediate	H-Poor
H	0.925	0.500	$1.4 \times 10^{-5}$
He	0.072	trace	$4.0 \times 10^{-6}$
C	$8.2 \times 10^{-4}$	0.128	0.325
N	$2.6 \times 10^{-4}$	0.040	0.024
O	$1.9 \times 10^{-3}$	0.304	0.651
Ne	$1.3 \times 10^{-4}$	trace	$2.4 \times 10^{-6}$
S	$2.4 \times 10^{-5}$	$3.8 \times 10^{-3}$	$5.1 \times 10^{-5}$

*Note:*

Abundances are all given as mole fractions.

## II. Intermediate Hydrogen Content Atmosphere

Our second case is one that falls midway between a hydrogen-rich atmosphere and one that has lost all of its hydrogen through escape processes. Here we choose a hydrogen abundance of 50% by volume. This hydrogen content could either be due to incomplete loss of accreted hydrogen or the result of outgassing of atmospheric material from the planetary surface. In this scenario the atmospheric chemistry remains mildly reducing, and the atmosphere is composed mostly of H<sub>2</sub>O, CO<sub>2</sub>, CH<sub>4</sub>, and N<sub>2</sub> in chemical equilibrium. Once again methane and ammonia are not expected to be photochemically stable in this atmosphere, and we present cases both with and without these molecules in what follows. For this scenario we have chosen an atmospheric mass equivalent to that of Earth's atmosphere.

## III. Hydrogen-Poor Atmosphere

For our final scenario, we take an atmosphere that has lost almost all of its atmospheric hydrogen over the planet's lifetime. For Gl 581c, whose surface should be too warm to host liquid water, the resulting atmospheric chemistry will be very similar to that of Venus. The oxidizing chemistry and the abundance of free carbon results in an atmosphere composed mostly of CO<sub>2</sub>. To keep with the comparison to Venus, we have also given this atmosphere a mass equal to Venus' atmospheric mass, or about 100 times greater than that of the Earth. For a Venusian atmosphere, photochemistry plays a role in aiding in the formation of sulfuric acid clouds via the reaction  $2\text{SO}_2 + \text{O}_2 + 2\text{H}_2\text{O} \rightarrow 2\text{H}_2\text{SO}_4$ . As long as the planet's atmosphere contains some SO<sub>2</sub> this process will occur, and under the right conditions this will result in a cloud layer on Gl 581c just like the one on Venus. Due to the uncertainties in the atmospheric abundance of H<sub>2</sub>SO<sub>4</sub>, in the following sections we present models both with and without sulfuric acid clouds for the hydrogen-poor scenario.

## 4. Results

### 4.1. Transmission Spectra as a Probe of Hydrogen Content

Our most significant finding is that transmission spectra are the best tool for distinguishing between hydrogen-dominated atmospheres and hydrogen-poor atmospheres. For a conceptual explanation, we can consider an exoplanet atmosphere to have a vertical

extent of  $10 H$ , where  $H$  is the scale height,

$$H = \frac{kT}{\mu_m g}. \tag{4.1}$$

The scale height is proportional to the inverse of the atmospheric mean molecular weight  $\mu_m$ , expressed from here on in terms of atomic mass units (u). In hydrogen-dominated atmospheres,  $\mu_m \simeq 2$ , and  $H$  is large. In contrast, in our hydrogen-poor atmosphere,  $\mu_m \simeq 40$ , so that the scale height, and hence the atmosphere available for transmission, is smaller by a factor of 20. Measuring the change in eclipse depth  $\Delta D$  across spectral lines in transmission gives the scale height according to

$$\Delta D \sim \frac{HR_{pl}}{R_*^2}. \tag{4.2}$$

This allows for a determination of  $\mu_m$  assuming that both the atmospheric temperature and surface gravity are known to within a factor of a few. Observations of spectral features in transmission should therefore offer a strong constraint on the atmospheric composition in terms of its hydrogen content. The sensitivity of scale height to atmospheric composition is illustrated in Figure 1.

In Figure 2 we have plotted our modeled spectra for each of the three cases of atmospheric composition that were discussed in Section 3. As expected from the scale height argument presented above, the hydrogen-rich atmosphere shows deep absorption features in transmission at a level of up to  $10^{-4}$ . The other two atmospheres have weaker features – by about a factor of 10. In the latter cases, due to the small scale height, the transmission spectrum only probes a very narrow range of height in the atmosphere.

Ideally, with the capability to detect transmission spectra at a level of less than a part in  $10^{-5}$  relative to the star, we could learn about the hydrogen content of a super-Earth atmosphere like Gl 581c. IR transmission spectroscopy would be the easiest way to differentiate between the various atmospheric cases. However, narrow-band photometry from Spitzer is currently the best that can be accomplished. In Figure 2 we also show the expected fluxes in each of the Spitzer IRAC bands and in the MIPS  $24\text{-}\mu\text{m}$  band for each model atmosphere. Each of the Spitzer bands averages over a number of spectral features, which effectively smooths out much of the transmission signal. However, there

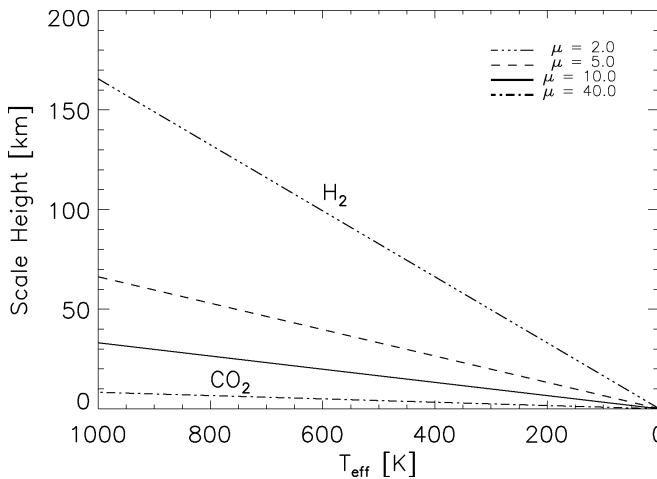


**Figure 1.** Atmospheric scale height as a function of effective temperature and for a variety of atmospheric compositions.

are perceptible changes from one channel to the next that could be suggestive of atmospheric composition and hydrogen content. In the case of the hydrogen-rich atmosphere, the expected Spitzer IRAC fluxes vary from band to band at a level of  $10^{-5}$ , while in the intermediate and hydrogen-poor cases this is reduced to a factor of  $10^{-6}$ . For other exoplanet systems the expected transmission signal will vary according to Eq. 4.2. If photometry at this level can be obtained, which will most probably need to wait for the launch of JWST, it will give observers a chance to place meaningful constraints on the atmospheric composition of super-Earths like Gl 581c.

#### 4.2. Thermal Emission Spectrum

The planetary emission spectrum can also be generally helpful in discerning the chemistry and composition of a Super-Earth atmosphere. We find that the three types of atmosphere that we explored for Gl 581c each reveal very different emission spectra. The observed features in a planet's emission spectrum represent the dominant sources of opacity in that atmosphere -  $\text{H}_2\text{O}$  for our hydrogen-dominated atmosphere,  $\text{CO}_2$  for the hydrogen-poor atmosphere, and a combination of both in the intermediate hydrogen content case. The spectral features are therefore a strong indicator of the chemistry at work in the planetary atmosphere. Figure 3 shows the wavelength-dependent emission calculated for each of the three cases of atmospheric composition. We have indicated the effect of methane and ammonia photochemistry on the emission spectra for the hydrogen-rich and intermediate cases, and the effect of a possible sulfuric acid cloud layer in the hydrogen-poor case.

To date, emission from extrasolar planets has been best measured through secondary eclipses observations of transiting systems. In Figure 4 we plot secondary eclipse depths for our three model atmospheres in the 1-30  $\mu\text{m}$  range. The expected eclipse depths

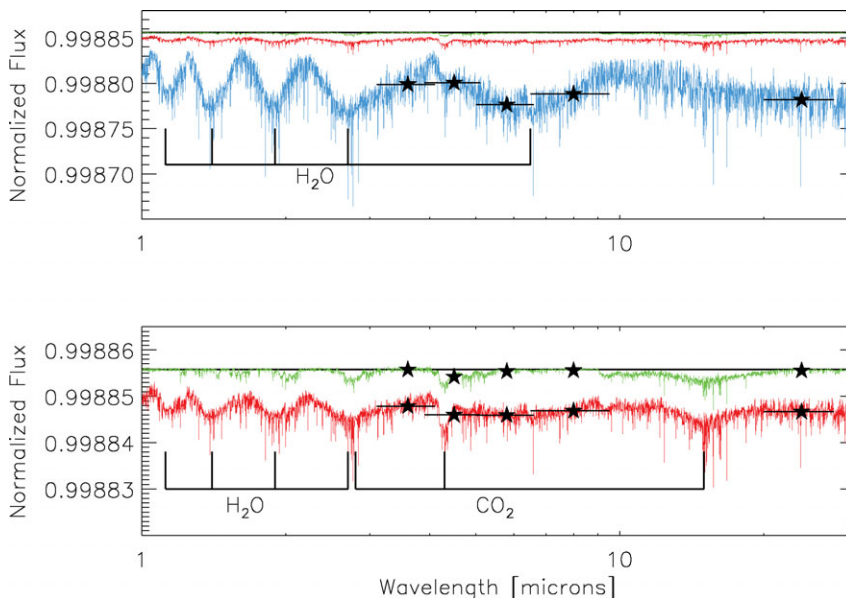


**Figure 2.** Top: Transmission spectra (transit flux divided by out-of-transit flux) of Gl 581c for the hydrogen-rich (blue), intermediate (red), and hydrogen-poor (green) atmospheres, along with no atmosphere (black line). The stars correspond to the relative flux that would be observed in each of the Spitzer IRAC bands as well as in the 24- $\mu\text{m}$  MIPS band, and the attached horizontal bars represent the width of each filter. Bottom: Same as above, but zoomed in to show the transmission spectra for the intermediate and hydrogen-poor atmospheres only.

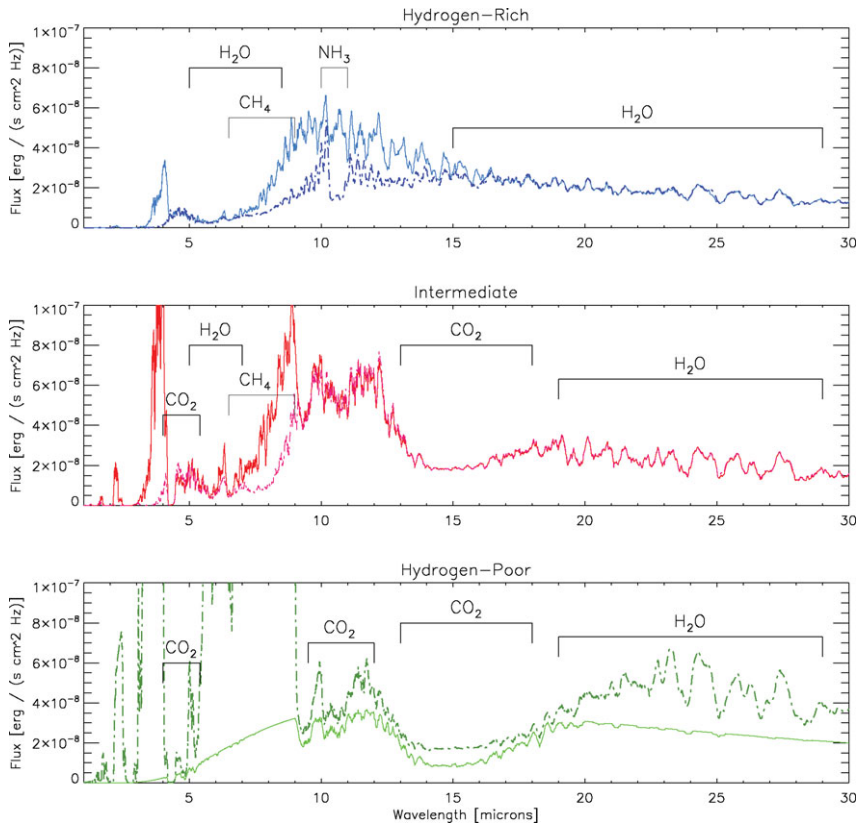


**Figure 3.** Emission spectra of Gl 581c for each of the three cases of atmospheric composition considered in this paper. In the top two panels, the solid lines are the spectra with  $\text{NH}_3$  and  $\text{CH}_4$  removed due to photochemical considerations. The dashed lines show the same spectra but for an atmosphere in chemical equilibrium. The bottom panel shows the hydrogen-poor emission spectra for a cloud-free model (dashed line) and a model with sulfuric acid clouds at a temperature of 400 K (solid line).

for Gl 581c in the IR are all predicted to be less than 70 ppm with the exception of the cloud-free hydrogen-poor model. In Figure 4 we also show the expected secondary eclipse depths in each of the Spitzer IRAC bands and in the MIPS 24  $\mu\text{m}$  band. The IRAC bands would give good coverage of water features in both the hydrogen-rich and intermediate atmospheres, however the expected eclipse depths are quite small at less than 10 ppm. In terms of constraining the nature of the planet's atmosphere, the detection of water features in the 1 - 10  $\mu\text{m}$  range and the  $\text{CO}_2$  feature in the 12-19  $\mu\text{m}$  range would be highly indicative of the atmospheric chemistry at work. Unfortunately, detecting spectral features from secondary eclipse observations would necessitate observations with a precision of better than  $10^{-5}$ , which is unlikely with currently available observing facilities.

## 5. Discussion

Currently, no transiting super-Earths have been detected. However, the CoRoT (Baglin 2003; Barge *et al.* 2005) and Kepler (Borucki *et al.* 2004; Basri *et al.* 2005) missions are both designed with the capability of detecting transiting super-Earths orbiting Sun-like stars. Additionally, ground-based transit surveys such as MEarth (Nutzman &

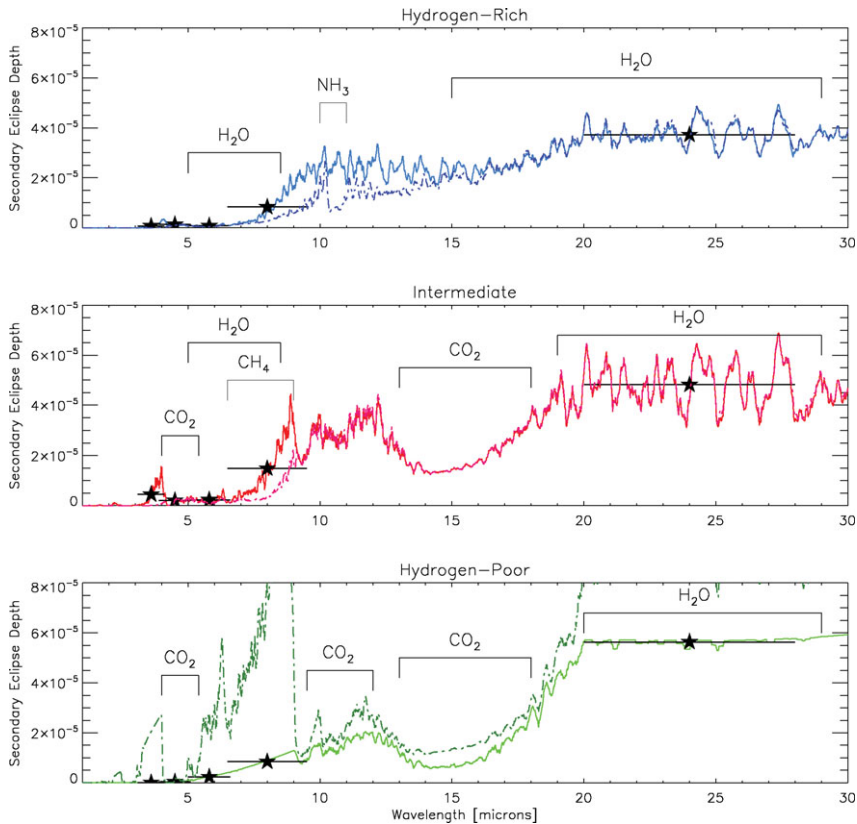


**Figure 4.** Secondary eclipse depths for the three atmosphere scenarios. Dashed lines in the top two panels represent models with methane and ammonia removed due to photochemical considerations. In the bottom panel we include spectra for the hydrogen-poor atmosphere both with (solid line) and without (dashed line) sulfuric acid clouds. The fluxes for the solid-line spectra averaged over the four Spitzer IRAC bands and the 24- $\mu\text{m}$  MIPS band are indicated by stars.

Charbonneau 2007), which will specifically target M-dwarfs, as well as radial velocity surveys both have the capabilities to detect planets in the super-Earth range. Most interestingly, the combination of these searches should allow for super-Earths to be found in a wide range of orbits and around a variety of types of stars.

While it is possible that Spitzer or Hubble will still allow for detections of atmospheric transmission or emission from a transiting Super-Earth, it is more likely that JWST (Gardner *et al.* 2006) will be the first to make these types of measurements at the precision needed. With its expected instrument complement, JWST should allow for follow-up observations of super-Earth atmospheres. Valenti *et al.* (in prep.) have simulated JWST NIRSpec spectra for transiting Earth-like planets orbiting M-stars, using atmospheric models from Ehrenreich *et al.* (2006). Scaling their results to the hydrogen-rich case for Gl 581c implies a 20-hour integration time and 6 transits needed to detect its transmission features with their expected depth of  $10^{-4}$ . These types of observations should be feasible with proper telescope scheduling and should allow for constraints to be placed on the nature of their atmospheres, and for the full richness of super-Earth atmospheres of different sizes, compositions, and orbits to be explored.



## References

- Baglin, A. 2003, *Advances in Space Research*, 31, 345
- Barge, P., Baglin, A., Auvergne, M., Buey, J.-T., Catala, C., Michel, E., Weiss, W. W., Deleuil, M., Jorda, L., Moutou, C., & COROT Team. 2005, in SF2A-2005: Semaine de l'Astrophysique Française, ed. F. Casoli, T. Contini, J. M. Hameury, & L. Pagani, 193
- Basri, G., Borucki, W. J., & Koch, D. 2005, *New Astronomy Review*, 49, 478
- Beaulieu, J.-P., Bennett, D. P., Fouque, P., Williams, A., Dominik, M., Jorgensen, U. G., Kubas, D., Cassan, A., Coutures, C., Greenhill, J., & *et al.* 2006, *Nature*, 439, 437
- Borucki, W., Koch, D., Boss, A., Dunham, E., Dupree, A., Geary, J., Gilliland, R., Howell, S., Jenkins, J., Kondo, Y., and 3 coauthors, 2004, in ESA SP-538: Stellar Structure and Habitable Planet Finding, ed. F. Favata, S. Aigrain, *A&A* Wilson, 177–182
- Brodbeck, C., Nguyen, V.-T., Bouanich, J.-P., Boulet, C., Jean-Louis, A., Bezard, B., & de Bergh, C. 1991, *J. Geophys. Res.*, 96, 1749
- Chevallier, L., Pelkowski, J., & Rutily, B. 2007, *Journal of Quantitative Spectroscopy and Radiative Transfer*, 104, 357
- Ehrenreich, D., Tinetti, G., Lecavelier Des Etangs, A., Vidal-Madjar, A., & Selsis, F. 2006, *A&A*, 448, 379
- Elkins-Tanton, L. & Seager, S. 2008, *ApJ*, submitted
- Fortney, J. J., Marley, M. S., & Barnes, J. W. 2007, *ApJ*, 659, 1661
- Freedman, R. S., Marley, M. S., & Lodders, K. 2007, ArXiv e-prints, 706
- Gardner, J. P., Mather, J. C., Clampin, M., Doyon, R., Greenhouse, M. A., Hammel, H. B., Hutchings, J. B., Jakobsen, P., Lilly, S. J., Long, K. S., and 13 coauthors, 2006, *Space Science Reviews*, 123, 485
- Hansen, B. M. S. 2007, *ApJS*, submitted
- Hunten, D. M., Donahue, T. M., Walker, J. C. G., & Kasting, J. F. 1989, *Escape of atmospheres and loss of water (Origin and Evolution of Planetary and Satellite Atmospheres)*, 386–422
- Nutzman, P. & Charbonneau, D. 2007, ArXiv e-prints, 709, 345
- Partridge, H. & Schwenke, D. W. 1997, *J. Chem. Phys.*, 106, 4618
- Rivera, E. J., Lissauer, J. J., Butler, R. P., Marcy, G. W., Vogt, S. S., Fischer, D. A., Brown, T. M., Laughlin, G., & Henry, G. W. 2005, *ApJ*, 634, 625
- Rothman, L. S., Jacquemart, D., Barbe, A., Benner, D. C., Birk, M., Brown, L. R., Carleer, M. R., Chackerian, C., Chance, K., Coudert, and 20 coauthors, 2005, *Journal of Quantitative Spectroscopy and Radiative Transfer*, 96, 139
- Seager, S., Kuchner, M., Hier-Majumder, C., & Militzer, B. 2007, ArXiv e-prints, 707
- Seager, S., Whitney, B. A., & Sasselov, D. D. 2000, *ApJ*, 540, 504
- Sotin, C., Grasset, O., & Mocquet, A. 2007, *Icarus*, 191, 337
- Udry, S., Bonfils, X., Delfosse, X., Forveille, T., Mayor, M., Perrier, C., Bouchy, F., Lovis, C., Pepe, F., Queloz, D., & Bertaux, J. . 2007, ArXiv e-prints, 704
- Valencia, D., Sasselov, D. D., & O'Connell, R. J. 2007, ArXiv e-prints, 704
- White, W. B., Johnson, S. M., & Dantzig, G. B. 1958, *J. Chem. Phys.*, 28, 751